JACS
JOURNAL OF THE AMERICAN CHEMICAL SOCIETY
Article
pubs.acs.org/JACS

Size-Dependent Dissociation of Carbon Monoxide on Cobalt Nanoparticles

Anders Tuxen,[†] Sophie Carenco,[†] Mahati Chintapalli,[†,‡] Cheng-Hao Chuang,[§,∥] Carlos Escudero,[†] Elzbieta Pach,[†] Peng Jiang,[†] Ferenc Borondics,[†] Brandon Beberwyck,[†,⊥] A. Paul Alivisatos,[†,⊥] Geoff Thornton,[†,#] Way-Faung Pong,[∥] Jinghua Guo,[§] Ruben Perez,[†] Flemming Besenbacher,[▽] and Miquel Salmeron*[,†]

[†]Material Sciences Division, Lawrence Berkeley National Laboratory, 1 Cyclotron Road, Berkeley, California 94720, United States
[‡]Department of Materials Science and Engineering, University of California, Berkeley, California 94720, United States
[§]Advanced Light Source, Lawrence Berkeley National Laboratory, 1 Cyclotron Road, Berkeley, California 94720, United States
[∥]Department of Physics, Tamkang University, Tamsui, Taiwan 250, R. O. C.
[⊥]Department of Chemistry, University of California, Berkeley, California 94720, United States
[#]London Centre for Nanotechnology and Department of Chemistry, University College London, 20 Gordon Street, London WC1H 0AJ, U.K.
[▽]Interdisciplinary Nanoscience Center (iNANO) and Department of Physics and Astronomy, Aarhus University, DK-8000 Aarhus C, Denmark

ABSTRACT: In situ soft X-ray absorption spectroscopy (XAS) was employed to study the adsorption and dissociation of carbon monoxide molecules on cobalt nanoparticles with sizes ranging from 4 to 15 nm. The majority of CO molecules adsorb molecularly on the surface of the nanoparticles, but some undergo dissociative adsorption, leading to oxide species on the surface of the nanoparticles. We found that the tendency of CO to undergo dissociation depends critically on the size of the Co nanoparticles. Indeed, CO molecules dissociate much more efficiently on the larger nanoparticles (15 nm) than on the smaller particles (4 nm). We further observed a strong increase in the dissociation rate of adsorbed CO upon exposure to hydrogen, clearly demonstrating that the CO dissociation on cobalt nanoparticles is assisted by hydrogen. Our results suggest that the ability of cobalt nanoparticles to dissociate hydrogen is the main parameter determining the reactivity of cobalt nanoparticles in Fischer–Tropsch synthesis.

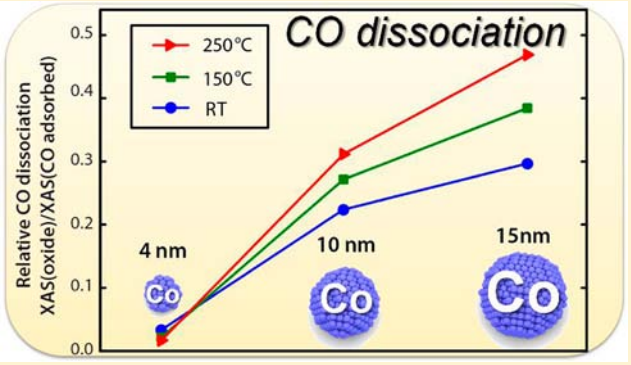

INTRODUCTION

Fischer–Tropsch synthesis (FTS) is an attractive way to produce liquid hydrocarbons as an alternative to fuels derived from crude oil. In FTS, metallic particles of Ni, Fe, Ru, or Co constitute the active phase for the reduction of CO by H_2. The detailed atomic-scale mechanism in the FT reaction has been and is still being discussed extensively in the literature.[1] One of the main controversies in FTS is related to the initial step where the CO molecule adsorbs and dissociates on the surface of the metal catalyst. Fischer and Tropsch originally proposed the *carbide mechanism*, wherein CO undergoes direct dissociation upon adsorption, resulting in C and O adspecies.[2−6] Recently this model has been supported by ab initio density functional theory (DFT) calculations on high Miller index Ru and Co surfaces.[7,8] However, another model suggests that the dissociation of CO is *hydrogen-assisted* in the sense that hydrogen adsorbed on the catalyst facilitates the dissociation of the triple bond of CO.[9−11] In this case, the dissociation goes through a −COH, −HCO, or $-H_2CO$ intermediate, which lowers the activation energy for CO dissociation.[12] Experimentally, the hydrogen-assisted model has been supported by the results of Ojeda and co-workers, who measured the kinetic isotope effect on the reaction rate.[13,14] Alternatively, a CO insertion mechanism producing formate on the surface was proposed,[26] but the role of these species in product formation was not asserted.[27] One of the main reasons why controversies about the CO dissociation mechanism still exist is that the surface species involved are extremely difficult to identify experimentally because they are short-lived and thus are present in very small concentrations on the surface of the particles. Moreover, the detection of these surface species requires surface science techniques capable of operating in situ under high pressure and high temperature.

Received: October 26, 2012
Published: January 22, 2013

   dx.doi.org/10.1021/ja3105889 | *J. Am. Chem. Soc.* 2013, 135, 2273−2278

Another central question in FTS is the influence of the size of the nanoparticles on the reactivity. It is well-known that the intrinsic reactivity of both Co and Ru nanoparticles is relatively constant in the 10−15 nm size regime, but decreases rapidly when the particle size is reduced below 8 nm. However, the fundamental principles underlying this size effect are still under debate.[15−19]

In this work, we used in situ X-ray absorption spectroscopy (XAS) to study Co nanoparticles in the 4−15 nm size regime at pressures of up to 1 atm. We present direct spectroscopic evidence showing that the dissociation of CO on cobalt nanoparticles is assisted by hydrogen. Moreover, our results reveal that the dissociation of CO is closely linked to the size of the nanoparticles, since larger Co nanoparticles dissociate CO much more effectively than smaller ones. Our results suggest that ineffective dissociation of hydrogen is responsible for the reduced reactivity of the smallest cobalt nanoparticles in FTS.

EXPERIMENTAL SECTION

The XAS experiments were performed on beamline 7.0.1 at the Advanced Light Source (Berkeley, CA) using an energy resolution of 0.2 eV on both the Co L-edge and the O K-edge, except for the experiments presented in Figure 5, which were done on beamline 6.3.1 with an energy resolution of 0.5 eV. All of the measurements were recorded in the total-electron-yield detection mode, making the XAS measurements sensitive to the first few nanometers of the samples. We used a specially designed gas cell with a ∼100 nm thick Si_3N_4 nitride window separating the high-pressure reactor volume from the beamline.[20] The sample was heated using a 975 nm IR fiber-optic laser that heats the gold foil coated with nanoparticles. The nanoparticles were prepared by colloidal chemistry methods according to ref 21. The nanoparticles were deposited on the gold foil using the Langmuir−Blodgett technique. Extensive care was taken to prevent the formation of nickel carbonyls, and all parts in the reactor cell that would come into contact with CO were constructed from copper- or gold-coated components. All of the measurements were conducted in flow mode with a flow rate of 40 mL/min for the reactive gas. Scanning electron microscopy (SEM) using a Zeiss Gemini Ultra-55 instrument was performed on the cobalt nanoparticles both before and after the XAS measurements.

RESULTS AND DISCUSSION

To study the adsorption of CO on cobalt nanoparticles as a function of particle size, we employed the cobalt nanoparticles depicted in the SEM images in the upper panel of Figure 1, which all displayed narrow size distributions. Before being exposed to CO, the nanoparticles were oxidized in situ under 1 atm O_2 at 200 °C for 5 min to remove all carbon impurities from the particles. The bottom spectrum in the lower panel of Figure 1 shows the Co L-edge for the 10 nm Co nanoparticles after this treatment. The peak at 780 eV and the shoulder at 778.5 eV reveal that the cobalt nanoparticles were in the Co_3O_4 state after the oxidation treatment. The gas flow was then switched to 1 atm H_2 at room temperature (RT). This reduced the nanoparticles to CoO (Figure 1, second spectrum from the bottom), as shown by the features at 776.5 and 781 eV.[22] Further annealing to 250 °C in H_2 reduced the nanoparticles completely to metallic Co, as revealed by the single asymmetric absorption peak at 778.0 eV (top spectrum). The Co nanoparticles were thus reduced in the sequence $Co_3O_4 \rightarrow CoO \rightarrow Co^0$ as observed in ref 23. We observed similar behavior for the 4 and 15 nm particles (data not shown), which were also completely reduced to metallic Co at 250 °C.

After reducing the nanoparticles to the metallic state in H_2, we exposed them to 1:1 (by flow rate) CO/He (1 atm) at RT

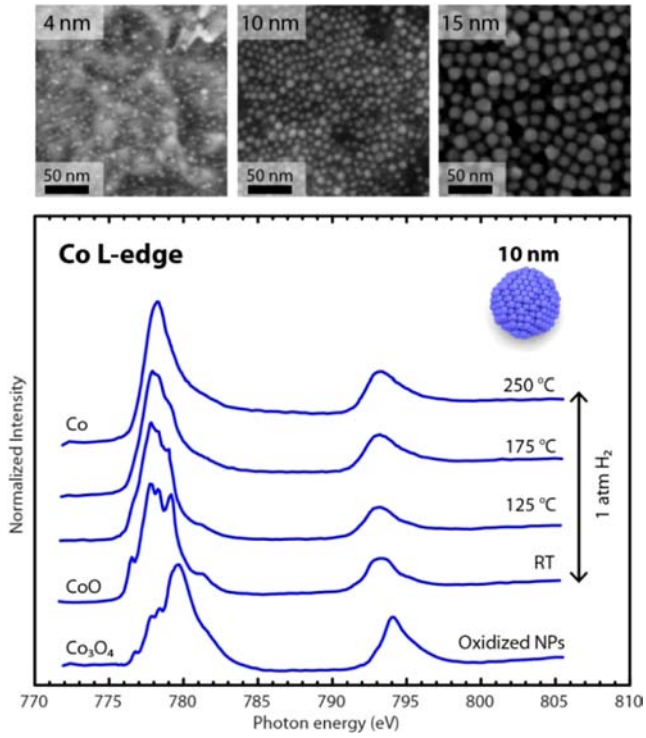

Figure 1. (top) SEM images of the 4, 10, and 15 nm cobalt nanoparticles used in this study. (bottom) XAS spectra of the Co L-edge during the reduction of the 10 nm nanoparticles in pure H_2 at increasing temperature.

for 5 min. We then replaced the CO/He mixture with pure He to avoid any contribution to the XAS spectra from gas-phase CO. The spectrum in the left panel of Figure 2 shows the O K-edge XAS results for the 4, 10, and 15 nm nanoparticles. The spectrum of the 15 nm nanoparticles at RT reveals XAS peaks that are typical of CO adsorbed on cobalt. In particular, an intense π^* transition at 534.2 eV and a weak σ^* transition at 550 eV were observed.[19] We assign these features to CO molecules adsorbed molecularly on the cobalt nanoparticles. However, there is also a clear XAS peak at approximately 531 eV that cannot be assigned to molecular CO. Instead, the energy of this peak is very close to that of the X-ray absorption edge of the bulk cobalt oxides CoO and Co_3O_4, as confirmed by comparison to the O K-edge of bulk oxide references (data not shown). This oxide peak is rather broad and may therefore arise from a mixture of the two oxides; we thus refer to it as the CoO_x peak. The formation of a surface oxide under these conditions was further confirmed by the XAS spectra on the Co L-edge (Figure 2, right panel). Here, the spectrum taken after exposure to CO/He at RT clearly shows small XAS features at 776.5, 779, and 781 eV. The formation of this CoO_x phase is even more clearly seen for the particles annealed to 250 °C under CO/He, after which very clear features from the surface oxide were observed on both the O K-edge and the Co L-edge.

The formation of this surface oxide on the cobalt nanoparticles in the presence of pure CO directly shows that a substantial fraction of the CO molecules undergo dissociative adsorption, producing surface oxygen and carbon. This does not exclude the possibility that other processes such as CO insertion could occur on the surface at the same time, although the resulting species could not be observed here. Interestingly, we found that the intensity of the oxide peak, and thus the tendency for CO to dissociate, depends directly on the actual size of the nanoparticles,

dx.doi.org/10.1021/ja3105889 | J. Am. Chem. Soc. 2013, 135, 2273−2278

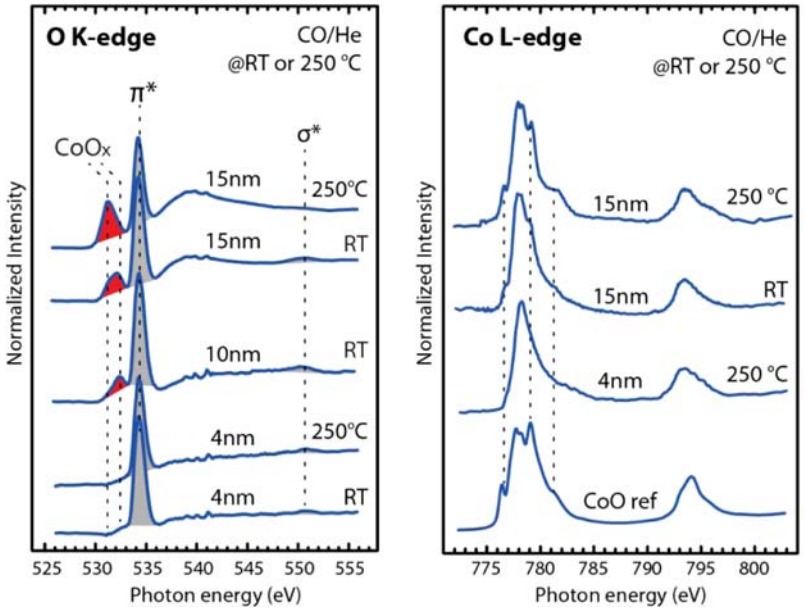

Figure 2. (left) O K-edge for reduced 4, 10, and 15 nm cobalt nanoparticles after exposure to 1:1 CO/He at RT and 250 °C. (right) Co L-edge for 4 and 15 nm nanoparticles under the same conditions as for the O K-edge.

as shown in the left panel of Figure 2. The oxide peak is very pronounced for the 15 nm nanoparticles but is smaller for the 10 nm nanoparticles and essentially undetectable for the 4 nm nanoparticles both at RT and at 250 °C, which is in agreement with the results reported in ref 19. These observations are directly supported by the measurements on the Co L-edge (Figure 2, right panel), which showed no oxide formation on the 4 nm nanoparticles (even at 250 °C), in contrast to the 15 nm nanoparticles, where oxide formation was clearly seen. By measuring the area of the surface oxide peak relative to that of the π^* peak in the O K-edge XAS spectra, we can estimate the relative amounts of oxide and remaining CO molecules on the nanoparticles and thus the ability of the nanoparticles to dissociate CO. Figure 3 shows these values for the 4, 10, and 15 nm

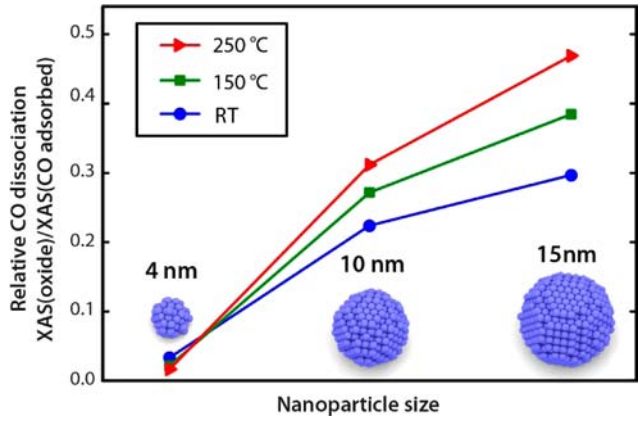

Figure 3. Relative concentration of dissociated CO species on 4, 10, and 15 nm nanoparticles after exposure to CO/He at different temperatures. The relative concentration was calculated as the ratio of the areas of the oxide XAS peak and the π^* peak from intact adsorbed CO.

cobalt nanoparticles after exposure to the CO/He mixture at RT, 150 °C, and 250 °C. It can be seen that the relative amount of oxide versus adsorbed molecular CO depends directly on the nanoparticle size: no dissociation occurs on the smallest (4 nm) nanoparticles, while a substantial fraction of the adsorbed CO molecules undergoes dissociation on the largest (15 nm) nanoparticles. Figure 3 also reveals that there is a clear increase in the oxide proportion with temperature, indicating that the oxide formation and thus the CO dissociation is a thermally activated process.

To gain further understanding of why the smallest nanoparticles display a very low ability to dissociate CO, we again exposed the 4 nm particles successively to CO/He and then pure He. At RT and 250 °C (Figure 4a,b, respectively), we observed again that the CO remains intact and molecularly adsorbed on the nanoparticles in the presence of He. Hence, there is no dissociation of CO in the absence of hydrogen. We subsequently switched the gas flow to pure H_2 and immediately observed a clear adsorption peak at 531.0 eV, which can be assigned to dissociated CO species, as discussed previously. The photon energy of this peak is not consistent with water, which is a byproduct of the FT reaction and thus may have formed when the adsorbed CO molecules are exposed to H_2. In addition, since the measurements were performed in flow mode, any water in the reactor would have been removed from the reactor volume.[19] Figure 4c reveals how the area of the oxide peak increases when the adsorbed CO is exposed to H_2. The experimental data thus show that the addition of H_2 immediately leads to dissociation of the adsorbed CO molecules, thus supporting the hydrogen-assisted CO dissociation mechanism discussed in the Introduction as opposed to the direct dissociation pathway.

In Figure 4d, we show the area of the CO π^* peak as a function of time at RT, 150 °C, and 250 °C. On the basis of these measurements, we calculate for the 4 nm NPs an activation energy of 23.7 kJ/mol for the hydrogen-assisted dissociation of CO in H_2 using the Arrhenius equation. This value, which is substantially lower than the activation energy for the formation of methane (90−100 kJ/mol),[19] shows that CO dissociation, while important, is not the rate-limiting step in the formation of methane under these conditions. Moreover, this value is significantly lower than the values computed for a

dx.doi.org/10.1021/ja3105889 | J. Am. Chem. Soc. 2013, 135, 2273−2278

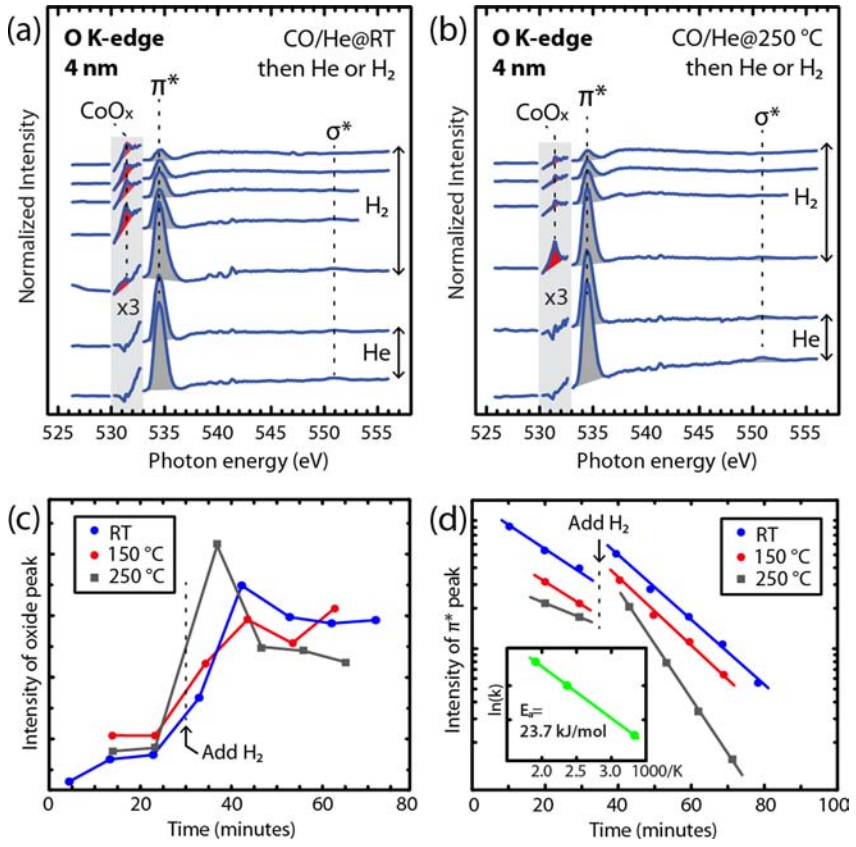

Figure 4. (a, b) O K-edge spectra of 4 nm particles after exposure to CO/He followed by pure He and then pure H_2 at (a) RT and (b) 250 °C. The time between each spectrum was approximately 10 min. (c, d) Areas of the (c) CoO_x and (d) π^* peaks as functions of time are shown for three different temperatures. The logarithmic ordinate scale in this case should be noted. The inset in (d) shows an Arrhenius plot obtained using the slopes of the previous curves, indicating an activation energy of 23.7 kJ/mol for the hydrogen-assisted CO dissociation.

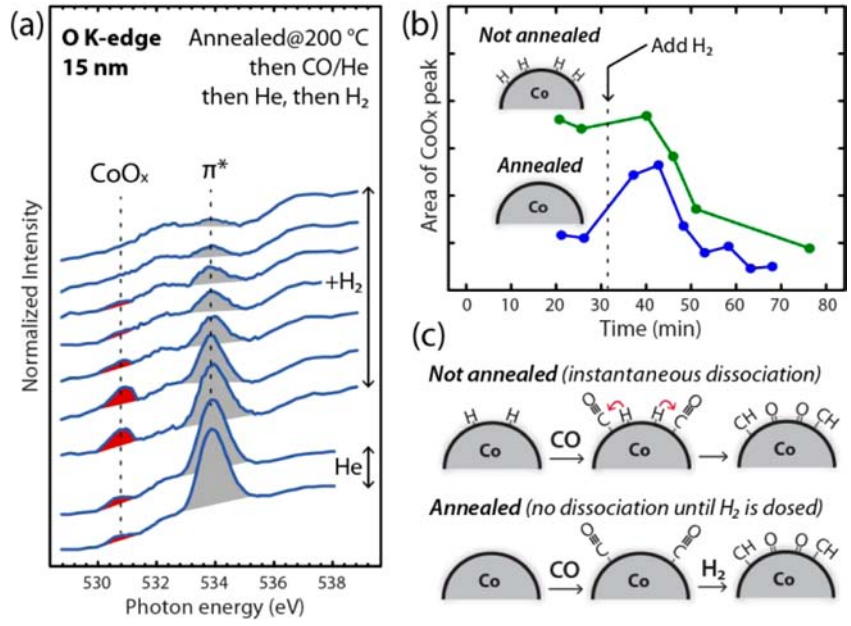

Figure 5. (a) O K-edge spectra of 15 nm cobalt nanoparticles after preannealing in He at 200 °C and subsequent exposure to CO/He and then H_2. (b) Areas of the CoO_x peaks from dissociation experiments on nanoparticles with (blue points) and without preannealing (green points). (c) Schematic illustration of CO dissociation in the two different experiments.

Co(0001) surface (90 and 68 kJ/mol for HCO and H_2CO formation, respectively),[25] highlighting the likely role of steps and defects in the CO dissociation process.

The observation that CO dissociation is assisted by hydrogen provides a direct explanation for the size-dependent dissociation that we observed on the 4, 10, and 15 nm particles.

dx.doi.org/10.1021/ja3105889 | J. Am. Chem. Soc. 2013, 135, 2273−2278

Herranz et al.[19] demonstrated that the ability of Co nanoparticles to dissociate hydrogen decreases with the particle size. In particular, H−D exchange experiments conducted on reduced Co NPs suggested that the increase in turnover frequency for CH_4 formation with 3−10 nm NPs could be linked with the increase in H_2 dissociation activity. Accordingly, the amount of dissociated hydrogen on the surface of the nanoparticles is expected to be substantially higher on the largest nanoparticles compared with the smallest particles, meaning that more hydrogen is available to assist the dissociation of CO on the largest particles. This explains the trend in Figure 3 that larger nanoparticles dissociate CO more effectively.

To obtain further proof that hydrogen adsorbed on the surface of the nanoparticles is responsible for the dissociation of CO, we performed an experiment in which the 15 nm nanoparticles were preannealed to 200 °C in He for 10 min before exposure to CO to remove adsorbed hydrogen from the surface of the nanoparticles. The two spectra at the bottom of Figure 5a reveal that the large nanoparticles in this experiment displayed little ability to dissociate CO, as evidenced by the very low amount of CoO_x. However, when the nanoparticles were exposed to H_2, the oxide peak increased substantially, revealing that the dosed hydrogen induces the dissociation of CO. Figure 5b shows the area of the oxide peak for the experiment with the preannealed nanoparticles (Figure 5a) along with that for a control experiment in which the nanoparticles were not preannealed. It is clearly seen that CO dissociated immediately when the nanoparticles were not preannealed (green points), while dissociation did not occur on the preannealed nanoparticles until H_2 was dosed (blue points). These experiments clearly confirm that residual hydrogen adsorbed on the surface of the nanoparticles is responsible for the dissociation of CO even on the larger nanoparticles.

The lower coverage of dissociated hydrogen on the small nanoparticles is expected not only to reduce the ability of the nanoparticles to dissociate CO but also to slow the further reaction of the CH_x fragments produced from the dissociation. This is in good agreement with the SSTIKA experiments performed by den Breejen et al.,[17] who found an increase in the surface residence time for CH_x on cobalt nanoparticles smaller than 6 nm. Also, the coverage of CH_x on the surface on the particles was found to decrease with particle size, which can be explained by a reduced CO dissociation rate due to a smaller amount of dissociated hydrogen. Carballo et al.[24] observed a similar effect on Ru nanoparticles, which they explained in terms of stronger adsorption of CO due to the larger d-orbital local density of states in the smaller particles and thus the larger degree of back-bonding between d orbitals and the antibonding π^* orbital in the CO molecule, which strengthens the Ru−C bond. However, stronger binding of CO does not alone explain our results, since stronger adsorption would weaken the C−O bond and thus lead to an increase in CO dissociation with decreasing cluster size. In fact, in our experiments we observed the opposite effect, since smaller particles display a reduced tendency to dissociate CO. Instead, the reduced tendency to dissociate CO with decreasing particle size must be an effect of the reduced ability of the particles to dissociate H_2, which is a necessary first step. The reaction pathway of the adsorbed hydrogen with adsorbed CO is still unclear, as is its indirect effect on the adsorption energy of the different species. Dedicated DFT modeling will be required to elucidate the size-dependent H-assisted CO dissociation mechanism and to identify the reaction intermediates.

SUMMARY

By studying cobalt nanoparticles with in situ soft X-ray absorption spectroscopy, we have demonstrated that the dissociation of CO is facilitated by hydrogen. Our experimental data thus support the hydrogen-assisted model. We suggest that the dissociation occurs through a −COH or $-CH_xO$ intermediate, although such intermediates were not directly identified by XAS. We also observed a clear size-dependent ability of the nanoparticles to dissociate CO, with smaller nanoparticles favoring molecular adsorption of CO and larger nanoparticles favoring CO dissociation. Importantly, our results indicate that it is the ability of the nanoparticles to dissociate hydrogen that determines their ability to dissociate CO via the hydrogen-assisted mechanism. This explains the well-known effect that the intrinsic reactivity in FTS decreases when the nanoparticle size decreases below 10 nm.

AUTHOR INFORMATION

Corresponding Author

mbsalmeron@lbl.gov

Notes

The authors declare no competing financial interest.

ACKNOWLEDGMENTS

This work was supported by the Director, Office of Science, Office of Basic Energy Sciences, Chemical Sciences, Geosciences, and Biosciences Division, under Department of Energy Contract DE-AC02-05CH11231. The authors further acknowledge User Proposal 994 at the Molecular Foundry and the Advanced Light Source for allocated beamtime. A.T. gratefully acknowledges the postdoc stipend "In-Situ Investigations of Nanoparticles for Fischer−Tropsch Catalysis" from the Danish Research Council for Independent Research | Natural Sciences. G.T. acknowledges support from the EPSRC (U.K.). R.P. acknowledges the financial support of the Spanish MEC (Project PR2011-0402), Fundación CajaMadrid and the UAM-Banco Santander Program of Collaboration with the USA. This material is based upon work supported by the National Science Foundation Graduate Research Fellowship under Grant No. DGE1106400.

REFERENCES

(1) Shetty, S.; van Santen, R. A. *Catal. Today* **2011**, *171*, 168.
(2) Fischer, F.; Tropsch, H. *Brennst.-Chem.* **1930**, *11*, 489.
(3) Fischer, F.; Tropsch, H. *Brennst.-Chem.* **1926**, *7*, 97.
(4) Schulz, H. *Appl. Catal., A* **1999**, *186*, 3.
(5) Davis, B. H. *Catal. Today* **2009**, *141*, 25.
(6) Bell, A. T. *Catal. Rev.* **1981**, *23*, 203.
(7) Shetty, S.; Jansen, A. P. J.; van Santen, R. A. *J. Am. Chem. Soc.* **2009**, *131*, 12874.
(8) Shetty, S.; van Santen, R. A. *Phys. Chem. Chem. Phys.* **2010**, *12*, 6330.
(9) van Helden, P.; van den Berg, J. A.; Ciobica, I. M. *Catal. Sci. Technol.* **2012**, *2*, 491.
(10) Blyholder, G.; Lawless, M. *Langmuir* **1991**, *7*, 140.
(11) Inderwildi, O. R.; Jenkins, S. J.; King, D. A. *J. Phys. Chem. C* **2008**, *112*, 1305.
(12) Andersson, M. P.; Abild-Pedersen, F.; Remediakis, I. N.; Bligaard, T.; Jones, G.; Engbæk, J.; Lytken, O.; Horch, S.; Nielsen, J. H.; Sehested, J.; Rostrup-Nielsen, J. R.; Nørskov, J. K.; Chorkendorff, I. *J. Catal.* **2008**, *255*, 6.
(13) Ojeda, M.; Li, A. W.; Nabar, R.; Nilekar, A. U.; Mavrikakis, M.; Iglesia, E. *J. Phys. Chem. C* **2010**, *114*, 19761.
(14) Ojeda, M.; Nabar, R.; Nilekar, A. U.; Ishikawa, A.; Mavrikakis, M.; Iglesia, E. *J. Catal.* **2010**, *272*, 287.

(15) Yang, J.; Tveten, E. Z.; Chen, D.; Holmen, A. *Langmuir* **2010**, *26*, 16558.
(16) Prieto, G.; Martinez, A.; Concepcion, P.; Moreno-Tost, R. *J. Catal.* **2009**, *266*, 129.
(17) den Breejen, J. P.; Radstake, P. B.; Bezemer, G. L.; Bitter, J. H.; Froseth, V.; Holmen, A.; de Jong, K. P. *J. Am. Chem. Soc.* **2009**, *131*, 7197.
(18) Bezemer, G. L.; Bitter, J. H.; Kuipers, H. P. C. E.; Oosterbeek, H.; Holewijn, J. E.; Xu, X. D.; Kapteijn, F.; van Dillen, A. J.; de Jong, K. P. *J. Am. Chem. Soc.* **2006**, *128*, 3956.
(19) Herranz, T.; Deng, X. Y.; Cabot, A.; Guo, J. G.; Salmeron, M. *J. Phys. Chem. B* **2009**, *113*, 10721.
(20) Escudero, C.; Jiang, P.; Pach, E.; Borondics, F.; West, M. W.; Tuxen, A.; Chintapalli, M.; Carenco, S.; Guo, J.; Salmeron, M. *J. Synchrotron Radiat.* **2013**, in press.
(21) Puntes, V. F.; Krishnan, K. M.; Alivisatos, A. P. *Science* **2001**, *291*, 2115.
(22) Morales, F.; de Groot, F. M. F.; Glatzel, P.; Kleimenov, E.; Bluhm, H.; Havecker, M.; Knop-Gericke, A.; Weckhuysen, B. M. *J. Phys. Chem. B* **2004**, *108*, 16201.
(23) Tsakoumis, N. E.; Voronov, A.; Ronning, M.; van Beek, W.; Borg, O.; Rytter, E.; Holmen, A. *J. Catal.* **2012**, *291*, 138.
(24) Carballo, J. M. G.; Yang, J.; Holmen, A.; Garcia-Rodriguez, S.; Rojas, S.; Ojeda, M.; Fierro, J. L. G. *J. Catal.* **2011**, *284*, 102.
(25) Zhuo, M.; Tan, K. F.; Borgna, A.; Saeys, M. *J. Phys. Chem. C* **2009**, *113*, 8357.
(26) (a) Pichler, H.; Schulz, H. *Chem. Ing. Tech.* **1970**, *42*, 1162. (b) Schweicher, J.; Bundhoo, A.; Kruse, N. *J. Am. Chem. Soc.* **2012**, *134*, 16135.
(27) Schweicher, J.; Bundhoo, A.; Frennet, A.; Kruse, N.; Daly, H.; Meunier, F. C. *J. Phys. Chem. C* **2010**, *114*, 2248.